Development/Plasticity/Repair

Functional Genomic Analysis of Remyelination Reveals Importance of Inflammation in Oligodendrocyte Regeneration

Heather A. Arnett,[1,2]* Ying Wang,[1,3]* Glenn K. Matsushima,[2,3] Kinuko Suzuki,[2,4] and Jenny P.-Y. Ting[1,2,3]

[1]Lineberger Comprehensive Cancer Center, [2]Neuroscience Center, and Departments of [3]Microbiology–Immunology and [4]Pathology and Laboratory Medicine, University of North Carolina, Chapel Hill, North Carolina 27599

Tumor necrosis factor α (TNFα), a proinflammatory cytokine, was shown previously to promote remyelination and oligodendrocyte precursor proliferation in a murine model for demyelination and remyelination. We used Affymetrix microarrays in this study to identify (1) changes in gene expression that accompany demyelination versus remyelination and (2) changes in gene expression during the successful remyelination of wild-type mice versus the unsuccessful attempts in mice lacking TNFα. Alterations in inflammatory genes represented the most prominent changes, with major histocompatibility complex (MHC) genes dramatically enhanced in microglia and astrocytes during demyelination, remyelination, and as a consequence of TNFα stimulation. Studies to examine the roles of these genes in remyelination were then performed using mice lacking specific genes identified by the microarray. Analysis of MHC-II-null mice showed delayed remyelination and regeneration of oligodendrocytes, whereas removal of MHC-I had little effect. These data point to the induction of MHC-II by TNFα as an important regulatory event in remyelination and emphasize the active inflammatory response in regeneration after pathology in the brain.

Key words: **oligodendrocytes; glia; neuroinflammation; regeneration; major histocompatibility complex; gene array; multiple sclerosis; remyelination; demyelination; TNF**

Introduction

Inflammation in the CNS is thought to be an exacerbating factor for many neurodegenerative and demyelinating disorders, most notably multiple sclerosis (MS). Many products of inflammation are seen in the plaques of patients with MS and have been proposed to contribute to the destruction of white matter (Brosnan and Raine, 1996; Sriram and Rodriguez, 1997; Raine et al., 1998); however, a protective role for neuroinflammation and inflammatory cytokines such as tumor necrosis factor α (TNFα) has emerged recently in models of demyelination and traumatic brain injury (Eugster et al., 1999; Scherbel et al., 1999; Suvannavejh et al., 2000; Juedes and Ruddle, 2001; Arnett et al., 2002). In addition, the deletion of TNFα in mice caused susceptibility to an immune-mediated demyelination model (Korner et al., 1997; Liu et al., 1998; Kassiotis et al., 1999). The ability of TNFα to generate multiple and sometimes opposing effects (exacerbatory, protective, or regenerative) can be attributed in part to the presence of its two receptors, TNFR1(p55) and TNFR2(p75) (Locksley et al., 2001). In an autoimmune demyelinating model, TNFR1 has been shown to be involved primarily in the initiation of demyelination, whereas TNFR2 often appears either uninvolved or yields a protective effect (Eugster et al., 1999; Suvannavejh et al., 2000; Kassiotis and Kollias, 2001). Using a neurotoxicant (cuprizone) to induce demyelination and study remyelination, we demonstrated previously that TNFα promotes remyelination and oligodendrocyte regeneration through TNFR2 (Arnett et al., 2001).

In agreement with these preclinical studies implicating TNFα in the amelioration of demyelinating disease, the use of anti-TNF therapy in patients with MS caused disease exacerbation, and its use in patients with rheumatoid arthritis resulted in new demyelinating lesions and new-onset MS (Lenercept Group, 1999; Mohan et al., 2001; Robinson et al., 2001; Sicotte and Voskuhl, 2001). A better understanding of the observed ability of TNFα to promote remyelination may lead to effective therapeutic interventions in the treatment of demyelinating diseases. Furthermore, because TNFα-null mice are defective in their ability to remyelinate, they provide a unique model for identifying factors important to this process.

To analyze global changes that occur during demyelination, remyelination, and TNFα-directed remyelination in the cuprizone model, we now use Affymetrix cDNA microarrays to identify (1) genes that accompany demyelination versus remyelination and (2) gene differences in wild-type and TNFα-null to compare successful versus unsuccessful remyelination. The latter are especially interesting because they should include differences that are critical to the regeneration of myelin and oligodendrocytes.

Our findings show alterations in genes involved in such diverse functions such as cell division, signaling, transcription, and development, although the largest category of genes upregulated during both demyelination and remyelination relates to inflam-

Received March 31, 2003; revised July 25, 2003; accepted July 29, 2003.

This work was supported by National Institutes of Health Grants NS34190 (J.P.-Y.T.) and NS24453 (K.S.) and National Multiple Sclerosis Society Grant RG1785 (J.P.-Y.T.).

*H.A.A. and Y.W. contributed equally to this work.

Correspondence should be addressed to Heather A. Arnett, Dana-Farber Cancer Institute, Smith Building 1070, Harvard Medical School, One Jimmy Fund Way, Boston, MA 02115. E-mail: heather_arnett@dfci.harvard.edu.

 0270-6474/03/239824-09$15.00/0

mation and the immune response. A number of candidate genes that may be involved in the inflammation-driven regeneration of oligodendrocytes are downstream of TNFα during successful remyelination. We chose major histocompatibility complexes (MHCs) I and II for further analysis because the expression patterns of both were enhanced significantly during remyelination and altered by TNFα. Furthermore, both MHC-I and -II are known to be present in demyelinating and remyelinating plaques of patients with multiple sclerosis, (Olsson, 1992).

Materials and Methods

Mice. C57BL/6J control mice were purchased from Jackson Laboratories (Bar Harbor, ME). MHC-I-deficient B2m$^{-/-}$ mice (*B2m*^{tm1Unc}) were purchased from Jackson Laboratories, previously backcrossed 11 times to a C57BL6/J background (Koller et al., 1990). MHC-II$^{-/-}$ mice (lacking Aβ) were bred in-house and backcrossed eight times to a C57BL6/J background (Grusby et al., 1991). TNF$\alpha^{-/-}$ mice were backcrossed nine times to a C57BL6/J background at Memorial Sloan-Kettering Cancer Center and maintained in our animal facility at University of North Carolina for testing (Marino et al., 1997). All animal procedures were conducted in pathogen-free conditions with complete compliance to the National Institutes of Health *Guide for the Care and Use of Laboratory Animals* and were approved by the Institutional Animal Care and Use Committee of the University of North Carolina at Chapel Hill.

Induction of demyelination and remyelination. To induce demyelination, male mice, 8–10 weeks old, were fed a diet of milled Purina mouse chow containing 0.2% cuprizone (Sigma, St. Louis, MO) for up to 6 weeks. Remyelination was initiated by returning the mice to a normal diet after 6 weeks of cuprizone (Morell et al., 1998; Matsushima and Morell, 2001).

RNA isolation. Total RNA was isolated from a dissected region of the corpus callosum of wild-type and TNF$\alpha^{-/-}$ mice at several points in treatment. RNA isolation was performed using the Qiagen RNeasy kit under RNase-free conditions (Qiagen, Valencia, CA). Purity was determined by A260/A280, by denaturing agarose gel electrophoresis, and by negative results after PCR for genomic contamination.

Microarray analysis. To profile gene expression differences, we used Affymetrix GeneChip arrays in which sets of oligonucleotides are immobilized on a chip and then hybridized with labeled RNA. These experiments used the mouse genome U74Av2 chips containing gene probes for ~6000 genes in the Mouse Unigene database as well as ~6000 expressed sequence tags clusters. cDNA synthesis was performed with the Superscript II system (Invitrogen/BRL, Grand Island, NY) and *in vitro* transcription labeling with biotinylated UTP and CTP was performed according to the manufacturer's recommendations (Enzo Diagnostics, Farmingdale, NY). Amplified cRNA was purified on an affinity column (Qiagen), and the quality of the amplification was verified by denaturing agarose gel electrophoresis. cRNAs were fragmented and then hybridized to prewetted array chips. Chips were washed according to Affymetrix washing protocols and subsequently stained using a fluorochrome–avidin conjugate. The probe arrays were scanned with the GeneChip system confocal scanner (Affymetrix, Santa Clara, CA). For an individual gene, hybridization of cRNA to a set of perfectly matched oligonucleotide sequences versus hybridization to a set of single mismatch oligonucleotide sequences yields a signal that is reflective of the level of expression of that gene. Data generated were analyzed using Genespring software. To lend greater fidelity to the data, this experiment was repeated, each with an RNA pool of three mice per strain and over the three chosen time points.

Quantitative real-time RT-PCR. TaqMan 5′ nuclease real-time PCR assays were performed using an ABI Prism 7900 sequence-detection system (PE Applied Biosystems, Foster City, CA) in a 15 μl reaction with universal master mix (Life Technologies/ BRL), 200 nM target primers, and 100 nM probe. Primers were designed to span intron–exon junctions to differentiate between cDNA and genomic DNA. The primers and probe used to detect mouse MHC-II (IA of b haplotype) were as follows: 5′ primer, GAGCATCCCAGCCTGAAGA; 3′ primer, CGATGCCGCTCAACATCTT; probe, Fam-ACTCAGACTGTGCCCTC CACTCCA-Tamra. The primers and probe for mouse MHC-I (H2D of b haplotype) were 5′ primer, GCTCCTCACTTCCACACTGAGA; 3′ primer, GGAAGAGCAGTCAGCGCTAGA; probe, Fam-AATAATTTGAATGTGGGTGGCTGGAGAGATG-Tamra. The primers and probe for mouse 18 S ribosomal RNA were 5′ primer, GCTGCTGGCACCAGACTT; 3′ primer, CGGCTACCACATCCAAGG; probe, Tet-CAAATTACCCACTCCCGACCCG-Tamra. Thermal cycle parameters were optimized to 2 min at 50°C, 2 min at 95°C, and 40 cycles comprising denaturation at 95°C for 15 sec and annealing–extension at 56°C for 1.5 min. Reactions for 18 S were performed during each experiment and used to normalize for amounts of cDNA. Presented results are representative of three separate trials, each performed in duplicate.

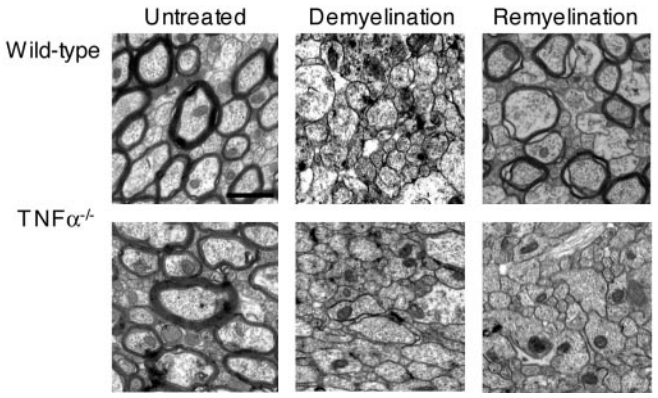

Figure 1. TNFα in remyelination. Electron microscopy was performed on cross-sections of the corpus callosum in wild-type and TNF$\alpha^{-/-}$ mice. Analysis is shown in untreated mice, after complete demyelination with the cuprizone, and after 2 weeks of remyelination. Scale bar, 2 μm.

Histology and electron microscopy. Animals were prepared for frozen, paraffin, and electron microscopy (EM) sections as described previously (Arnett et al., 2001). Paraffin sections were stained with luxol-fast blue (LFB)/periodic acid Schiff for myelin, glutathione *S*-transferase (GST-π) for mature oligdodendrocytes (Biotrin, Newton, MA; 1:500), RCA-1 for microglia (Vector, Burlingame, CA; 1:500), and GFAP for astrocytes (Dako, Carpinteria, CA; 1:100). We quantified immunopositive cells by counting positive cells within the median of the corpus callosum, confined to a 0.033 mm^2 area. Only those stained cells with an observable nucleus by DAPI stain or light microscopy were counted. Cell counts are presented as averages from at least six mice per time point. Frozen sections were stained for MHC-I (TIB126; American Type Culture Collection, Manassas, VA; 1:100) and MHC-II (PharMingen, San Diego, CA; 1:10) as well as the above antibodies for colocalization. EM ultrathin sections were stained with uranyl acetate and lead citrate as described (Coetzee et al., 1996).

Statistics. Data are expressed as mean ± SD. Comparisons were statistically evaluated using ANOVA followed by a Bonferonni *post hoc* analysis. Results were considered significant if $p < 0.05$.

Results

Remyelination in mice lacking TNFα

The use of cuprizone, a copper chelating agent delivered through the diet, causes demyelination that is predictable in pathology and time course. Removal of cuprizone for 1 week causes detectable remyelination that progresses with time. Using this model, we confirmed previous findings that the degree of myelination in the corpus callosum of TNF$\alpha^{-/-}$ and wild-type mice before cuprizone treatment is indistinguishable, as is their degree of demyelination and oligodendrocyte loss after an extended 5 weeks of cuprizone treatment (Arnett et al., 2001). Wild-type mice, however, underwent rapid remyelination after removal of cuprizone, whereas TNF$\alpha^{-/-}$ mice failed to remyelinate effectively (Fig. 1) (Arnett et al., 2001).

Table 1. Transcripts altered in demyelinated and remyelinating lesions

Accession #	Demyelination	Remyelination	Gene name
Cell Cycle or Proliferation-associated			
AF061503	1	-3	block of proliferation 1 (BOP1)
AW048937	5	1	Cdkn1a
M86183	37	29	Cyclin D3
X75888	1	-74	Cyclin E
X54149	3	7	GADD45; MyD118
J03482	3	2	histone H1
AF022110	AP	AP	Integrin beta-5
AV314625	2	3	POLA2; DNA polymerase alpha
Developmental			
D88792	-3	1	CRP2, double LIM protein-1
AV361541	1	-4	Crygd
X76292	1	-3	desert hedgehog
U13370	-8	1	Edg2; Lysophosphatidic acid receptor
AI842277	4	-3	IGF binding protein 3
AJ005621	2	4	LIM domain binding 3 (LDB3/Cypher)
M34094	5	1	Midkine; retinoic acid-responsive protein
Z49086	1	4	mouse developmental kinase 5 (MDK5)
AI841137	7	-5	Plexin B2
AB011030	1	-3	PRDC; BMP antagonist
U52824	2	3	rd5, tubby protein
AA866668	2	3	Sox3
AF053756	7	4	UNC-51-like kinase (ULK1)
AV246963	-6	1	Wnt1 responsive Cdc42 (Wrch1)
Immune or Stress Response			
Type A			
X67083	3	1	chop-10, ER stress
AB015224	AP	1	CMAP; leukocystatin
U27267	8	1	LIX, C-X-C chemokine precursor
AI852641	11	1	P8 stress responsive gene
L33412	3	1	RAGE
Type B			
AC002397	2	4	B-cell receptor-associated protein 37
X97227	3	2	CD53
AV248632	2	3	CISh; cytokine inducible SH2-containing protein
X58861	4	2	complement C1q A-chain
M22531	4	2	complement C1q B-chain
X66295	4	3	complement C1q C-chain
U77461	3	2	complement C3a receptor
X06454	3	3	complement C4
U41341	AP	AP	endothelial monocyte-activating polypeptide (EMAP)
AI854595	5	9	FKBP-rapamycin associated protein (FRAP/mTOR)
X02801	7	6	glial fibrillary acidic protein (GFAP)
U43086	6	3	glucocorticoid-attenuated response gene 49
M85078	1	3	GM-CSFR, CD116
U23778	6	3	hematopoietic-specific early-response A1-b
U23781	5	3	hematopoietic-specific early-response A1-d
X61597	AP	AP	kallikrein-binding protein
AV356071	4	2	Laptm5; retinoic acid-inducible E3 protein
D37837	9	6	L-fimbrin
X64224	10	12	Ly-42, CD23
AF024637	6	3	Ly83, DAP12, KARAP
M21050	AP	AP	lysozyme M
X51547	AP	AP	lysozyme P
X16834	AP	AP	Mac-2
AB007599	5	2	MD-1, associates with RP105
X01838	3	2	MHC beta-2 microglobulin
M18837	3	2	MHC beta-2-microglobulin
M69069	3	2	MHC class I H-2D
AI117211	6	5	MHC class I H-2K
M58156	20	12	MHC class I H-2K
M95514	AP	AP	MHC class II alpha chain
X00496	3	4	MHC invariant chain; CLIP
X16202	3	3	MHC Q4 class I antigen
J04491	3	2	MIP-1alpha, chemokine
L20315	5	3	Mpg-1; macrophage specific protein
X13986	13	5	osteopontin
X67809	11	5	peptidylprolyl isomerase (cyclophilin) C-associated
AF039601	1	3	TGF-beta type III receptor
Type C			
X04418	-9	-2	prolactin
L23636	PA	1	Ly72L, Flt3 ligand
AJ222714	-8	1	chemokine receptor CCR6
Lipid metabolism and transport			
Z22661	14	8	apolipoprotein C1
AA770736	7	1	Induced in fatty liver dystrophy 2 (Ifld2)
AA726364	6	2	Lipoprotein lipase
M63335	4	1	Lipoprotein lipase
X81627	67	23	lipocalin; 24p3 gene
Lysosome or Proteasome-related			
U74683	5	3	cathepsin C
U06119	4	2	cathepsin H
AJ242663	4	2	cathepsin Z
U22033	4	2	Lmp7, 20S proteasome subunit
AV327201	-4	-2	Man2b1, lysosomal alpha-mannosidase
AA638816	PA	-3	Psmb4; proteasome beta chain
AA414947	-25	1	Psmd11, 26S proteasome subunit
Myelin components			
Y07812	-3	1	Myelin and lymphocyte protein (MAL)
M31811	-4	1	myelin associated-glycoprotein (MAG)
M37335	-3	2	myelin proteolipid protein (PLP)
L20942	-6	2	myelin/oligodendrocyte glycoprotein (MOG)
Neuronal/Neurotransmission			
L42293	3	3	acyl-coenzyme A: cholesterol acyltransferase
AB005450	-4	1	carbonic anhydrase XIV (CA XIV)
AF019566	2	PA	hypocretin
D10651	3	4	NMDAR2B
X72966	AP	AP	Rab3A
X84239	3	5	Rab5B
AI430879	1	5	steroid sulfatase
AJ002306	3	3	synaptogyrin 1b
AV356394	1	-5	syntrophin-1
Signaling			
AF078112	-3	-11	calcium signal-modulating ligand (Calmg)
X14836	3	3	CAMKII alpha
X87142	4	4	CAMKII alpha
AF044602	1	PA	G protein-coupled receptor 66
Y15798	1	-3	G protein-coupled receptor kinase 6 (GRK6-B)
U02313	-2	-4	MAST205
AB015978	10	2	oncostatin M receptor beta
M55561	6	3	phosphatidylinositol-linked antigen (pB7)
AV159979	-2	-8	Pip5k2a; Phosphatidylinositol-4-phosphate 5-kinase
AI195478	1	-18	Pnkp; Polynucleotide kinase 3'- phosphatase
AW122076	-30	-4	Ppp1r1a; Protein phosphatase inhibitor
AV354894	-2	-3	Prkm8ip; protein kinase
AF020526	1	-3	SH2-B PH domain containing signaling mediator 1
D88187	-48	-18	PTPf , tyrosine phosphatase
AB014485	22	6	RA70; src kinase-associated phosphoprotein
Structural			
M12481	-2	-3	beta-actin
U28932	1	-4	calponin
AB012042	1	-4	keratin 6 beta
AF067180	3	2	Kif5c; kinesin heavy chain
U96723	1	3	myosin I beta
AJ005567	4	4	SPRR2I
X53753	PA	-2	tropomyosin 5
Transcription or Translation			
X00686	-3	-5	18S ribosomal RNA
U75530	1	-3	4E-BP2, PHAS-II
AB012276	14	1	ATFx
X61800	4	2	c /ebp delta
AB025015	4	3	elongin A
X15763	1	3	GATA-1, DNA-binding protein
X98207	3	1	Histone deacetylase 1 (HDAC1)
AF074882	1	3	Histone deacetylase 3 (HDAC3)
U57051	3	3	Hoxb13
U20735	3	3	junB
L27453	2	3	PBX1B
U37500	-4	1	RNA polymerase II largest subunit
U21226	AP	AP	Thing1/Hand1
AB020495	2	3	Vax1

Affymetrix gene chip analysis was performed on corpus callosum RNA from wild-type mice at time points representing normal levels of myelin, complete demyelination, and active remyelination. Gene expression data are presented for the demyelinated and remyelinating time points as fold changes above or below (shown in red as a negative value) the expression data for the untreated mice. Only those genes with a raw value of >1000 in at least one condition, an approximately threefold change in expression, and an SE of <0.4 of the normalized values in duplicate experiments were included for analysis. AP denotes that the expression of that gene was absent in untreated samples and present in treated samples; PA denotes that a gene went from present in untreated samples to absent in treated samples. Genes are grossly categorized according to their function, with genes of unknown function or functions other than those listed available as supplemental data (available at www.jneurosci.org). The immune and stress response genes are further divided according to their patterns of expression: Type A genes are upregulated after demyelination and recede during remyelination; type B genes are upregulated and stay upregulated during remyelination; type C genes are downregulated during demyelination.

Table 2. Genes altered in mice lacking TNFα after demyelination and during remyelination

Accession #	Demyelination	Remyelination	Gene name
Cell Cycle or Proliferation-associated			
U90267	-3	1	Cdk5r2; cyclin-dependent kinase
AF044336	1	PA	p16, Cdkn2a
X75888	-2	38	Cyclin E
AV291335	-2	-4	MCM5, replication licensing factor
AV130885	-5	1	Nap1l4; Nucleosome assembly protein 1-like 4
AV314625	-3	-4	POLA2; DNA polymerase alpha
D13546	-6	1	POLA2; DNA polymerase alpha
U53584	-3	1	POLG; DNA polymerase gamma
Developmental			
AV361541	-6	10	Crygd
AV360936	-11	1	Crybb2; betaB2-crystallin
U57720	AP	AP	Cryptic; EGF-related
U24160	1	PA	dishevelled 2
Y11245	1	PA	forkhead box M1 (Foxm1)
AF054623	6	1	Frizzled-1
X99104	-3	-18	Gli2
AF077659	1	-3	homeodomain-interacting protein kinase 2 (Hipk2)
X04480	3	5	insulin-like growth factor I
X71922	1	3	insulin-like growth factor II
U15159	1	-20	Lim kinase 1
Z27410	4	5	Lim homeobox protein 1 (Lim1)
X74040	PA	PA	forkhead box C2 (Foxc2)
D88792	3	3	CRP2, double LIM protein-1
U71125	1	3	Mesp2, Notch signaling pathway
AF016714	-2	-3	myeloid elf-1-like factor
D86948	-3	-3	plexin 1
U52824	1	-3	rd5; tubby protein
X97818	4	1	semaphorin G
AA866668	1	-3	Sox3
U61970	-3	1	Wnt10b
AV246963	-1	-4	Wnt1 responsive Cdc42 (Wrch1)
Immune or Stress Response			
AA050273	5	4	CCR11, chemokine receptor
AJ222714	1	-3	CCR6 gene; chemokine receptor
M28240	1	-9	CD19
U60473	-2	-3	CD59; complement inhibitory protein
X77952	1	-5	CD105; endoglin
J04946	1	3	CD143; angiotensin converting enzyme
AF042158	1	3	CIITA form III
M13926	3	2	granulocyte colony stimulating factor 3
AI132585	6	9	complement C1 receptor
AV272809	1	-4	Dhodh
AI854595	-48	-2	FKBP-rapamycin associated protein (FRAP/mTOR)
AV233170	-4	7	IFI4 interferon-activatable protein 204
X01973	1	8	IFN-alpha 4
U78299	1	-6	lipoxin A4 receptor
L23636	AP	2	Ly72L, Flt3 ligand
L38423	1	-3	Lymphotoxin-beta receptor
AB023418	-4	-2	MCP-2; cytokine
D90146	-4	-2	MHC class I Qa-2 cell surface antigen
M27134	-23	-3	MHC class I; H-2K
M95514	1	-5	MHC class II alpha chain
M35247	-2	-3	MHC class II, T region locus 17
X12760	3	1	Perforin
AF030001	1	-3	RAGE
L33412	-2	3	RAGE
X57796	AP	1	TNFR1
Neuronal/Neurotransmission			
AV356394	1	4	alpha1-syntrophin
AF039833	2	4	Caspr; neurexin IV
AF053724	-4	1	endobrevin; VAMP-8
AF098633	PA	-4	GLUT4 vesicle protein; vp115
X72966	PA	PA	Rab3A
D45207	2	3	syntaxin1B
AI326966	-4	1	urotensin II receptor
Signaling			
L12367	9	5	adenylyl cyclase-associated protein (CAP)
AV220336	-2	-3	cGMP-dependent protein kinase anchor (GKAP42)
M94450	-2	-3	EGFR-binding protein GRB7
U49853	1	-6	FLP1, HSCF; tyrosine phosphatase
U87965	1	-5	G-protein1
U85714	1	3	phospholipase C-beta-1b
AV249638	1	3	Phosphorylase B kinase gamma catalytic chain
AV367375	-3	PA	PKCzeta
AA408341	-6	5	PLA2g5; secretory phospholipase
AF030131	-4	2	Plenty of SH3s (POSH)
AF036535	1	-3	Prkaac; AMP activated protein kinase
AF020526	1	3	SH2-B PH domain containing signaling mediator 1
AI646422	1	-3	RIBP
Structural			
AJ130783	4	32	APC2
U28932	1	10	calponin; actin-binding protein
AB012042	1	4	keratin 6 beta
AJ005567	-2	-4	Small proline-rich protein 2i
X53753	AP	2	tropomyosin 5
Transcription or Translation			
X15763	1	-4	GATA-1
AB000096	-4	3	GATA-2
X83733	-3	PA	Gnrpx gene; splicing factor 3a
X98207	-3	PA	Histone deacetylase 1 (HDAC1)
AF074882	-3	-2	Histone deacetylase 3 (HDAC3)
Y11091	2	PA	map kinase interacting kinase (Mnk1)
Y11092	2	-10	map kinase interacting kinase (Mnk2)
AF004294	1	4	myelin transcription factor 1 (myt1)
U75530	1	4	PHAS-II
L03215	1	-4	PU.1, Spi-1
U37500	4	2	RNA polymerase II largest subunit
AI853032	1	5	Sfrs4 splicing factor
U21226	-3	PA	Thing1/Hand1

Affymetrix gene expression data from corpus callosum of wild-type mice were compared to that of TNF$\alpha^{-/-}$ mice with similar treatments. The data are shown for TNF$\alpha^{-/-}$ mice as fold changes above or below (shown in red as a negative value) their counterpart wild-type mice. Only those genes with a raw value of >1000 in at least one condition, an approximately threefold change in expression, and SE of <0.4 of the normalized values in duplicate experiments were included for analysis. AP denotes that the expression of that gene was absent in untreated samples and present in treated samples; PA denotes that a gene went from present in untreated samples to absent in treated samples. Genes are grossly categorized according to their function, with genes of unknown function or functions other than those listed available as supplemental data (available at www.jneurosci.org).

Transcripts altered in demyelinated and remyelinating lesions

To profile gene expression differences, we used Affymetrix GeneChip arrays in which sets of oligonucleotides were immobilized on a chip and then hybridized with labeled cDNA. Three time points were chosen: untreated, 5 weeks of cuprizone treatment (representing the complete demyelination of the corpus callosum), and 6 weeks of treatment followed by 1 week of recovery (7 weeks; representing active remyelination). Data were analyzed in duplicate by comparison-based analysis. Only those genes with a raw value of >1000 in at least one condition and a greater than threefold change in expression over control were included for analysis. The overall correlation coefficient between replicate samples ranged from 0.5 to 0.8, and for an individual gene to be included for analysis, the SE between replicates was required to be <0.4 of the normalized values. These relatively strict standards are likely to generate false-negative signals but less likely to produce false-positive signals.

As expected, demyelination and oligodendrocyte apoptosis lead to the rapid downregulation of oligodendrocyte- and myelin-related genes, as shown through the gene array analysis (Table 1). These include myelin–oligodendrocyte glycoprotein (MOG), myelin-associated glycoprotein (MAG), myelin proteolipid protein (PLP), and myelin- and lymphocyte-specific protein (MAL). Genes involved in diverse functions such as cell cycle, development, and signal transduction constitute large groups of altered genes; however, the largest category of genes altered during both demyelination and remyelination consists of inflammatory and stress-response genes (Table 1). The data underscore the massive inflammatory response mounted during demyelination and remyelination. Some of these include GFAP, a marker for astrogliosis, and markers for microglia–macrophage, which have been documented to be upregulated during cuprizone treatment (Hiremath et al., 1998). The two largest components of immune-related genes that were induced after demyelination are MHC- and complement-related genes. Cytokines, cytokine receptors, and other inflammatory mediators were enhanced. Multiple enzymes involved in lysosomes including cathepsins C, H, and Z and lysoszymes M and P were also upregulated. These proteolytic enzymes may be related to the increased microglia–macrophage phagocytosis of the disrupted myelin or to the processing of antigens by MHC-I and -II. Lysozymes are often considered markers of activated cells of monocytic origin and have been shown previously to correlate with the recruitment of microglia–macrophages after demyelination (Morell et al., 1998; Jurevics et al., 2002).

Two primary patterns of gene expression are observed among the immune genes shown in Table 1. In the group labeled Type A, the genes were upregulated during demyelination but then reversed to basal levels. In the group labeled Type B, the genes were upregulated during both demyelination and remyelination. Remarkably, most of the immune response genes belong to the latter. This suggests that the immune transcripts upregulated during remyelination do not represent a subset of the immune response but rather a more generalized effect. It also implicates inflammatory genes as important components of remyelination.

Transcripts altered in mice lacking TNFα

To identify genes that are involved in remyelination, it is important to compare gene expression profiles of mice that have undergone successful remyelination with those that have exhibited unsuccessful or delayed remyelination. The results with TNF$\alpha^{-/-}$ mice (Fig. 1) indicate that a comparison of these mice with wild-type mice during the remyelination phase should reveal genes that are putatively important for remyelination. Affymetrix analyses of cDNA from the corpus callosum of these two sets of mice were performed at the following time points: before cuprizone treatment, when demyelination was completed in both strains (5 weeks of cuprizone treatment), and when remyelination was substantial in the wild-type mice, but delayed in the TNF$\alpha^{-/-}$ mice (at 7 weeks, when cuprizone was removed for the last week).

In agreement with the histologic and pathologic analysis, TNF$\alpha^{-/-}$ and wild-type mice showed few differences in gene expression before cuprizone treatment (data not shown). In contrast, significant differences were found between TNF$\alpha^{-/-}$ and wild-type mice after demyelination as well as during remyelination (Table 2). Because TNF$\alpha^{-/-}$ mice showed defective remyelination at the week 7 time point, special emphasis was placed on these gene differences. The primary categories of genes that were expressed more highly in wild-type mice than TNF$\alpha^{-/-}$ mice during the remyelinating phase include immune response, signaling, and developmental and transcriptional regulation (Table 2). Notably several genes in the MHC family were reduced in mice lacking TNFα.

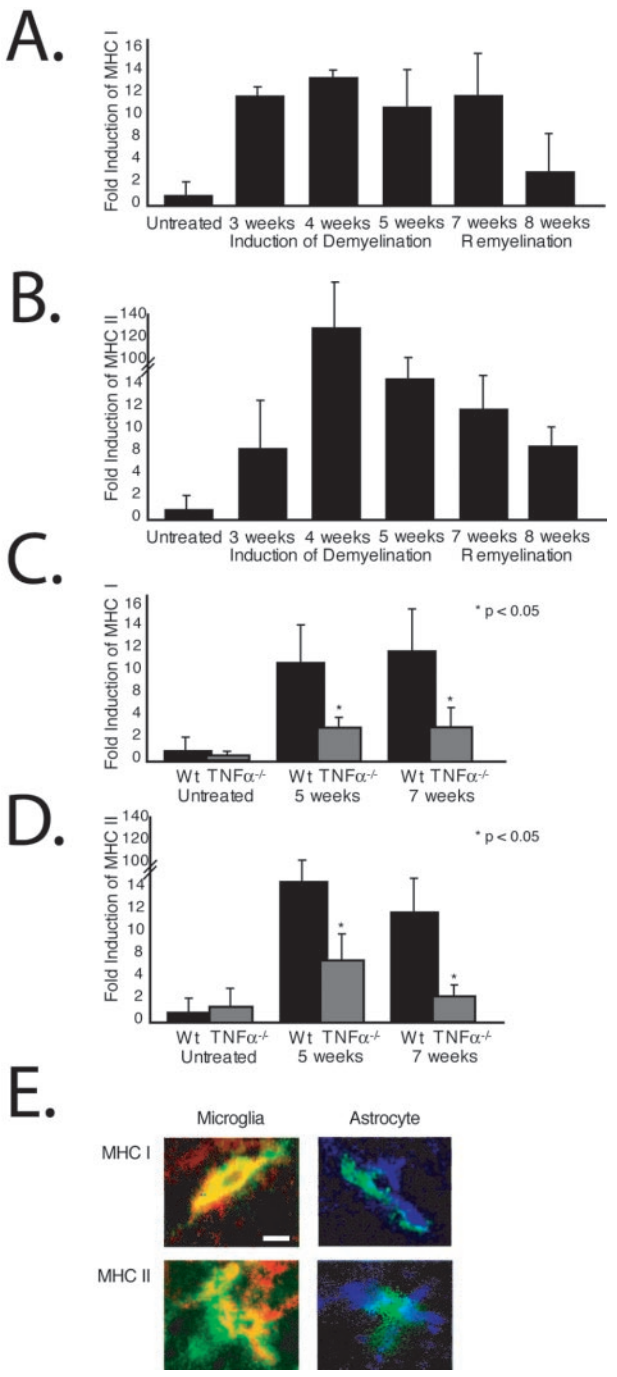

Figure 2. Expression of MHC-I and -II. *A*, *B*, Quantitative analysis of MHC-I and -II transcripts using quantitative real-time RT-PCR on total RNA isolated from the corpus callosum during demyelination and remyelination in wild-type mice. Each bar represents the averaged fold induction over untreated wild-type mice of at least three mice per genotype per time point ($\pm$SD). The scale is interrupted to accommodate the large value obtained for MHC-II with wild-type mice after 4 weeks of cuprizone treatment. *C*, *D*, Quantitative analysis of MHC-I and -II transcripts in wild-type mice compared with that in mice lacking TNFα. *$p < 0.05$. *E*, Antibodies were used to localize expression of MHC-I and -II (green) during demyelination of wild-type mice and colocalized to microglia (RCA-1, red) and astrocytes (GFAP, blue). Yellow indicates colocalization of the red and green fluorochromes. Scale bar, 12.5 μm.

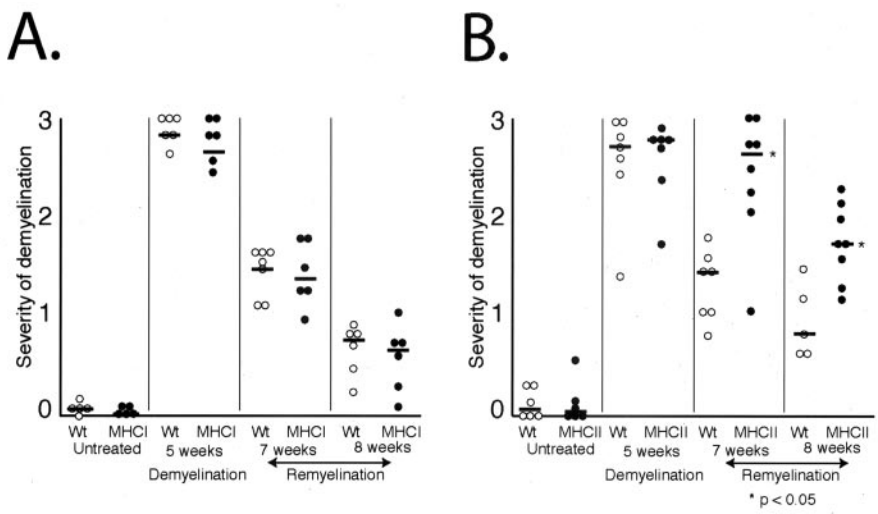

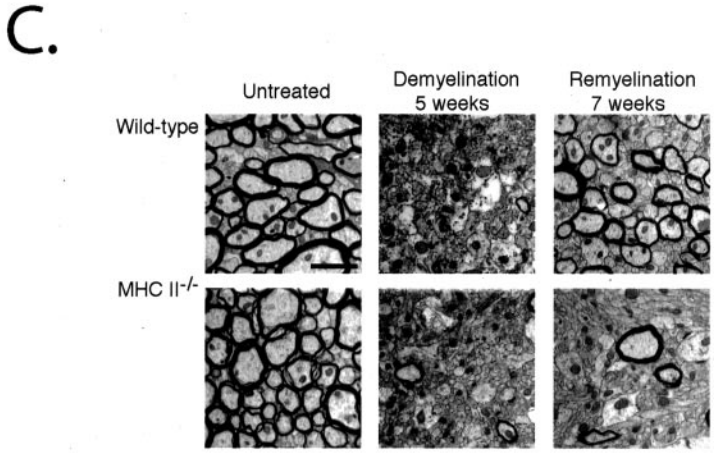

D.

	g-ratio	Percent unmyelinated fibers
Untreated		
Wild-type	0.717 +/- 0.032	0.6%
MHC II$^{-/-}$	0.748 +/- 0.014	0.5%
Treated for 5 weeks		
Wild-type	0.973 +/- 0.078	88.6%
MHC II$^{-/-}$	0.941 +/- 0.062	88.0%
Treated for 6 weeks + 1 week recovery		
Wild-type	0.816 +/- 0.036	31.5%
MHC II$^{-/-}$	0.923 +/- 0.042*	78.0%*

* p<0.001

Figure 3. MHC-I and -II in remyelination. *A*, *B*, Wild-type mice, MHC-I-null mice, and MHC-II-null mice were analyzed at various time points during demyelination and remyelination. Sections containing the corpus callosum at the level of the fornix were stained for LFB/PAS, and the corpus callosum was scored by three investigators on a scale of 0 (completely myelinated) to 3 (completely demyelinated), with the presence of blue fibers indicative of intact myelin. *$p < 0.05$. *C*, Remyelination was examined further with electron microscopy. Pictures represent a cross-section of the corpus callosum at the level of the fornix in untreated mice, mice completely demyelinated with cuprizone, and mice allowed to remyelinate for 1 week. Scale bar, 2 μm. *D*, *g*-ratios and percentage unmyelinated fibers were calculated from a minimum of 200 fibers per mouse per time point. *$p < 0.001$.

titative real-time RT-PCR at time points additional to those included in the Affymetrix analysis. This analysis shows similar patterns of increases in the transcription of MHC-I and -II during cuprizone-induced inflammation, with the peak of expression occurring at 4 weeks of cuprizone treatment (Fig. 2*A*,*B*). This time point correlates with the peak of microglia–macrophage infiltration into the corpus callosum (Hiremath et al., 1998). Elevated MHC-I and -II expression was maintained during remyelination, although the level decreased at the 8-week endpoint. Levels of MHC-I and -II were decreased after demyelination and remyelination in the absence of TNFα ($p < 0.05$) (Fig. 2*C*,*D*), although the degree of microglia–macrophage recruitment was similar in the wild-type and TNF$\alpha^{-/-}$ mice in this model (Arnett et al., 2001). Thus, transcription of both MHC-I and -II genes is induced by TNFα, but TNFα is not required for MHC gene expression because expression is still observed in TNF$\alpha^{-/-}$ mice. Detectable MHC-I (Fig. 2*E*, green) predominantly localizes to both microglia (red) and astrocytes (blue) in the demyelinating lesion. MHC-II is expressed primarily on microglia but also occasionally on astrocytes (Fig. 2*E*).

Roles of MHC-I and -II in remyelination

To perform functional genomic analysis, we characterized the roles of MHC-I and -II in remyelination using mice lacking expression of MHC-I or -II. The mice used to study the former lack B2m, which is essential for the expression of properly folded MHC-I protein (Koller et al., 1990). The mice used to study the latter lacked Aβ chain, which eliminates I-A expression (Grusby et al., 1991). Because of a natural defect in the Eα promoter of MHC II, this strain lacks all MHC-II expression. Untreated wild-type and MHC-I or -II null mice exhibited similar degrees of myelination before treatment (Fig. 3*A*, *B*, untreated). The degree of demyelination was determined by the extent of LFB staining and was read in a double-blind manner by three investigators. All three strains were also completely demyelinated after the extended 5 weeks of cuprizone treatment (Fig. 3*A*,*B*, 5 weeks). When the toxin was removed, wild-type mice and MHC-I$^{-/-}$ mice exhibited rapid remyelination within 1 week, which progressed steadily by 2 weeks (Fig. 3*A*, 7 and 8 weeks). In dramatic contrast, MHC-II$^{-/-}$ mice demonstrated a significant delay in remyelination ($p < 0.05$) (Fig. 3*B*, 7 and 8 weeks).

LFB analysis is a qualitatitve measurement of myelination. Ultrastructural analysis and quantitation by electron microscopic inspection represent much more accurate approaches to

Expression of MHC-I and -II during demyelination and remyelination

The considerable number of MHC-related genes that were enhanced during demyelination and remyelination in wild-type mice and their alteration by the absence of TNFα implicate a role for these genes in the control of remyelination. We verified expression of MHC-I and -II in this disease model through quan-

determine the extent of myelination in MHC-II$^{-/-}$ versus wild-type mice (Fig. 3*C*). A measurement of myelination, the *g*-ratio, was calculated as the ratio of the diameter of the axon to the diameter of the axon and surrounding myelin. Three mice from each group at each time point were tested, and a minimum of 200 fibers per mouse per strain per time point were measured. This provides an assessment of the percentage of unmyelinated axons throughout the treatment protocol in wild-type and MHC-II-null mice (Fig. 3*D*). A typical *g*-ratio for a normally myelinated axon is between 0.6 and 0.8, where a *g*-ratio of 1.0 is completely demyelinated. After 5 weeks of treatment, 88–89% of axons in the corpus callosum of wild-type and MHC-II$^{-/-}$ mice were completely demyelinated. Within 1 week of remyelination, 32% of wild-type axons remained demyelinated compared with 78% in MHC-II$^{-/-}$ mice.

During the demyelination process, mature oligodendrocytes in the corpus callosum undergo apoptosis (Mason et al., 2000). Remyelination is initiated with the reappearance of new myelinating oligodendrocytes in the lesion. The oligodendrocytes in wild-type and MHC-II$^{-/-}$ mice were depleted from the corpus callosum to similar degrees after 5 weeks of cuprizone treatment; however, after 1 week of recovery, wild-type mice had twofold more oligodendrocytes in the corpus callosum than MHC-II$^{-/-}$ mice ($p < 0.05$) (Fig. 4*A*,*B*). In contrast, the results with MHC-I$^{-/-}$ mice are indistinguishable from wild-type mice. This finding suggests that MHC-II is important in the regeneration of new oligodendrocytes and explains the delay in remyelination observed in mice lacking MHC-II.

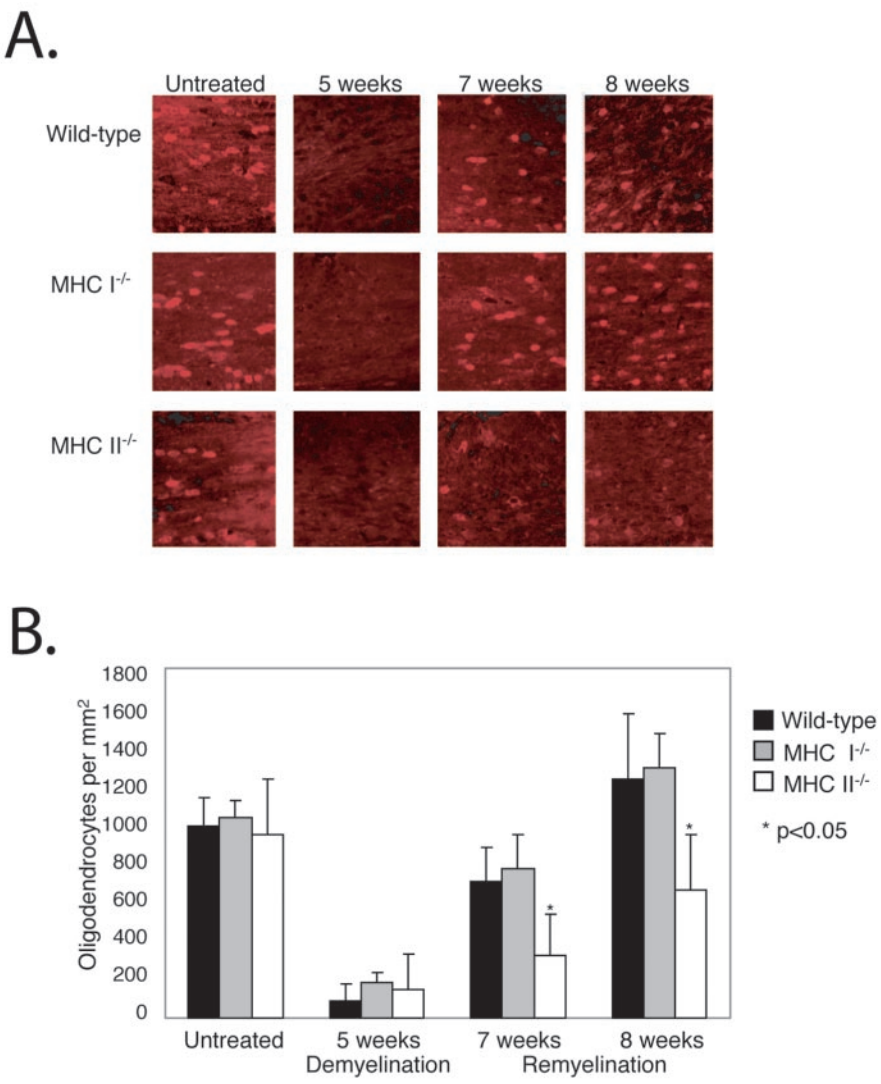

Figure 4. MHC-II and the regeneration of oligodendrocytes. *A*, Oligodendrocytes were identified during demyelination and remyelination in wild-type mice and mice lacking MHC-I or -II using an antibody to GST-Π (red). *B*, Quantification of oligodendrocytes in the corpus callosum. Each bar represents an average of the results of at least six mice per genotype per time point. *$p < 0.05$.

Discussion

In an effort to identify important factors in myelination, we have identified patterns of gene expression observed during cuprizone-induced demyelination and remyelination in wild-type mice. These were compared with TNF$\alpha^{-/-}$ mice, which showed retarded remyelination. Two of the most impressive findings are the predominance of immune and stress response genes during both demyelination and remyelination, and the significant effects of TNFα on inflammatory gene expression. In particular, MHC-II is upregulated during both demyelination and remyelination, is controlled by TNFα, and is important for the reappearance of new, myelinating oligodendrocytes required for successful remyelination. Interestingly, the genes for TNFα and MHC-II are proximal to each other, and they represent the only consistent linkages to MS susceptibility in humans (Fukazawa et al., 2000; Kantarci et al., 2002). Further study of MHC-II and other genes identified in this screen could establish them as important and novel therapeutic targets in demyelinating diseases.

Cuprizone is an ideal model for studying demyelination, remyelination, and the role of neuroinflammation. The induction of demyelination and remyelination is easy to administer, and the outcome is predictable in pathology and disease course. Administration of cuprizone to mice results in an impressive inflammatory reaction reflected by tremendous microglial accumulation and astrogliosis (Hiremath et al., 1998; Arnett et al., 2001; McMahon et al., 2001). In retrospect, it is not surprising that most of the genes upregulated after demyelination and during remyelination are involved in the inflammatory response. Remarkably, many of these immune response genes are related to the MHC family.

MHC-I and -II are increased under a wide range of pathologic conditions and play multiple roles during inflammation in the CNS (Neumann, 2001). In the brain, these factors have been most studied in the presentation of antigens in murine experimental autoimmune encephalitis in which demyelination follows the generation of myelin-reactive T lymphocytes. The presence of MHC-II has also been shown to be protective for regeneration and axon integrity in a mouse model of viral encephalitis (Njenga et al., 1999). Low levels of MHC-I are present on most cells and

function by presenting endogenous foreign peptides to CD8+ cells. Alternatively, MHC-II is present on professional antigen-presenting cells, including macrophages and dendritic cells, and presents exogenous antigenic peptides to CD4+ cells. Both microglia and astrocytes express MHC-II *in vitro*, but microglia appear to represent the predominant MHC-II-positive cells *in vivo*, similar to our observations in this study (Dong and Benveniste, 2001).

Although antigen presentation is a primary function of MHC-I and -II, a T lymphocyte infiltrate is not easily found in the cuprizone model, where the blood–brain barrier remains intact (Matsushima and Morell, 2001). Furthermore, the remyelination phase is independent of T cells as shown by the use of RAG$^{-/-}$ mice, which lack lymphocytes (Arnett et al., 2001). MHC-II has been previously hypothesized to have signaling functions in microglia and macrophages independent of T lymphocytes through its cytoplasmic domain. MHC-II has been demonstrated to contribute to the activation of microglia–macrophage in the brain in a model of Krabbes disease, in which lymphocytes are also not known to play a role (Matsushima et al., 1994). Future experiments will be directed at addressing the signaling potential of MHC-II in this model.

The use of gene array analysis has provided extraordinary insights regarding gene alterations during different permutations; however, the significance of functional genomics is underscored by the failure to find a role for MHC-I in the remyelination phase despite significant changes in this and related genes during demyelination, remyelination, and after TNFα deletion. The most straightforward possibility is that TNFα, a well known inducer of MHC-I (Panek et al., 1994; Neumann et al., 1997), obligatorily induces MHC-I, but this has no biologic consequences on the myelination process. Another possibility is that the enhanced levels of MHC-I have functions that are not revealed by our analysis. We have used mice lacking B2m, which might not be the same as a deletion of the gene for *MHC-I*, because expression of "empty" MHC-I can be forced on cells without B2m (Allen et al., 1986; Bix and Raulet, 1992). We are aware that previous studies of transgenic mice with MHC-I expression in oligodendrocytes have observed alterations in myelination (Turnley et al., 1991). In those studies, however, the expression of MHC-I is forced and on oligodendrocytes, which do not normally express MHC.

Although it is clear that TNFα and MHC-II are involved in the regeneration of oligodendrocytes and remyelination, the mechanism for the precise involvement of the immune system in remyelination is unclear. One possibility is that the expression of these inflammatory molecules causes the upregulation, either directly or indirectly, of factors that contribute to the proliferation and maturation of new progenitors. This study supports that hypothesis by showing an upregulation of multiple transcription factors and other proteins with known functions in the development of the CNS after the immune response to demyelination.

In summary, this study supports the possibility that inflammation has its use in the repair of demyelination, although not all immune-related molecules that are enhanced during remyelination appear to have a direct functional impact on this process. Sorting out the inflammatory processes that are beneficial versus those that may be harmful is crucial to the design of improved therapies for demyelinating or dysmyelinating disorders.

References

Allen H, Fraser J, Flyer D, Calvin S, Flavell R (1986) Beta 2-microglobulin is not required for cell surface expression of the murine class I histocompatibility antigen H-2Db or of a truncated H-2Db. Proc Natl Acad Sci USA 83:7447–7451.

Arnett HA, Mason J, Marino M, Suzuki K, Matsushima GK, Ting JP (2001) TNF alpha promotes proliferation of oligodendrocyte progenitors and remyelination. Nat Neurosci 4:1116–1122.

Arnett HA, Hellendall RP, Matsushima GK, Suzuki K, Laubach VE, Sherman P, Ting JP (2002) The protective role of nitric oxide in a neurotoxicant-induced demyelinating model. J Immunol 168:427–433.

Bix M, Raulet D (1992) Functionally conformed free class I heavy chains exist on the surface of beta 2 microglobulin negative cells. J Exp Med 176:829–834.

Brosnan CF, Raine CS (1996) Mechanisms of immune injury in multiple sclerosis. Brain Pathol 6:243–257.

Coetzee T, Fujita N, Dupree J, Shi R, Blight A, Suzuki K, Popko B (1996) Myelination in the absence of galactocerebroside and sulfatide: normal structure with abnormal function and regional instability. Cell 86:209–219.

Dong Y, Benveniste EN (2001) Immune function of astrocytes. Glia 36:180–190.

Eugster HP, Frei K, Bachmann R, Bluethmann H, Lassmann H, Fontana A (1999) Severity of symptoms and demyelination in MOG-induced EAE depends on TNFR1. Eur J Immunol 29:626–632.

Fukazawa T, Sasaki H, Kikuchi S, Hamada T, Tashiro K (2000) Genetics of multiple sclerosis. Biomed Pharmacother 54:103–106.

The Lenercept Multiple Sclerosis Study Group (1999) TNF neutralization in MS: results of a randomized, placebo-controlled multicenter study. Neurology 53:457–465.

Grusby MJ, Johnson RS, Papaioannou VE, Glimcher LH (1991) Depletion of CD4+ T cells in major histocompatibility complex class II-deficient mice. Science 253:1417–1420.

Hiremath MM, Saito Y, Knapp GW, Ting JP, Suzuki K, Matsushima GK (1998) Microglial/macrophage accumulation during cuprizone-induced demyelination in C57BL/6 mice. J Neuroimmunol 92:38–49.

Juedes AE, Ruddle NH (2001) Resident and infiltrating central nervous system APCs regulate the emergence and resolution of experimental autoimmune encephalomyelitis. J Immunol 166:5168–5175.

Jurevics H, Largent C, Hostettler J, Sammond DW, Matsushima GK, Kleindienst A, Toews AD, Morell P (2002) Alterations in metabolism and gene expression in brain regions during cuprizone-induced demyelination and remyelination. J Neurochem 82:126–136.

Kantarci OH, de Andrade M, Weinshenker BG (2002) Identifying disease modifying genes in multiple sclerosis. J Neuroimmunol 123:144–159.

Kassiotis G, Kollias G (2001) Uncoupling the proinflammatory from the immunosuppressive properties of tumor necrosis factor (TNF) at the p55 TNF receptor level. Implications for pathogenesis and therapy of autoimmune demyelination. J Exp Med 193:427–434.

Kassiotis G, Pasparakis M, Kollias G, Probert L (1999) TNF accelerates the onset but does not alter the incidence and severity of myelin basic protein-induced experimental autoimmune encephalomyelitis. Eur J Immunol 29:774–780.

Koller BH, Marrack P, Kappler JW, Smithies O (1990) Normal development of mice deficient in beta 2M, MHC class I proteins, and CD8+ T cells. Science 248:1227–1230.

Korner H, Riminton DS, Strickland DH, Lemckert FA, Pollard JD, Sedgwick JD (1997) Critical points of tumor necrosis factor action in central nervous system autoimmune inflammation defined by gene targeting. J Exp Med 186:1585–1590.

Liu J, Marino MW, Wong G, Grail D, Dunn A, Bettadapura J, Slavin AJ, Old L, Bernard CC (1998) TNF is a potent anti-inflammatory cytokine in autoimmune-mediated demyelination. Nat Med 4:78–83.

Locksley RM, Killeen N, Lenardo MJ (2001) The TNF and TNF receptor superfamilies: integrating mammalian biology. Cell 104:487–501.

Marino MW, Dunn A, Grail D, Inglese M, Noguchi Y, Richards E, Jungbluth A, Wada H, Moore M, Williamson B, Basu S, Old LJ (1997) Characterization of tumor necrosis factor-deficient mice. Proc Natl Acad Sci USA 94:8093–8098.

Mason JL, Jones JJ, Taniike M, Morell P, Suzuki K, Matsushima GK (2000) Mature oligodendrocyte apoptosis precedes IGF-1 production and oligodendrocyte progenitor accumulation and differentiation during demyelination/remyelination. J Neurosci Res 61:251–262.

Matsushima GK, Morell P (2001) The neurotoxicant, cuprizone, as a model to study demyelination and remyelination in the central nervous system. Brain Pathol 11:107–116.

Matsushima GK, Taniike M, Glimcher LH, Grusby MJ, Frelinger JA, Suzuki

K, Ting JP (1994) Absence of MHC class II molecules reduces CNS demyelination, microglial/macrophage infiltration, and twitching in murine globoid cell leukodystrophy. Cell 78:645–656.

McMahon EJ, Cook DN, Suzuki K, Matsushima GK (2001) Absence of macrophage-inflammatory protein-1alpha delays central nervous system demyelination in the presence of an intact blood-brain barrier. J Immunol 167:2964–2971.

Mohan N, Edwards ET, Cupps TR, Oliverio PJ, Sandberg G, Crayton H, Richert JR, Siegel JN (2001) Demyelination occurring during anti-tumor necrosis factor alpha therapy for inflammatory arthritides. Arthritis Rheum 44:2862–2869.

Morell P, Barrett CV, Mason JL, Toews AD, Hostettler JD, Knapp GW, Matsushima GK (1998) Gene expression in brain during cuprizone-induced demyelination and remyelination. Mol Cell Neurosci 12:220–227.

Neumann H (2001) Control of glial immune function by neurons. Glia 36:191–199.

Neumann H, Schmidt H, Cavalie A, Jenne D, Wekerle H (1997) Major histocompatibility complex (MHC) class I gene expression in single neurons of the central nervous system: differential regulation by interferon (IFN)-gamma and tumor necrosis factor (TNF)-alpha. J Exp Med 185:305–316.

Njenga MK, Murray PD, McGavern D, Lin X, Drescher KM, Rodriguez M (1999) Absence of spontaneous central nervous system remyelination in class II-deficient mice infected with Theiler's virus. J Neuropathol Exp Neurol 58:78–91.

Olsson T (1992) Immunology of multiple sclerosis. Curr Opin Neurol Neurosurg 5:195–202.

Panek RB, Lee YJ, Itoh-Lindstrom Y, Ting JP, Benveniste EN (1994) Characterization of astrocyte nuclear proteins involved in IFN-gamma- and TNF-alpha-mediated class II MHC gene expression. J Immunol 153:4555–4564.

Raine CS, Bonetti B, Cannella B (1998) Multiple sclerosis: expression of molecules of the tumor necrosis factor ligand and receptor families in relationship to the demyelinated plaque. Rev Neurol (Paris) 154:577–585.

Robinson WH, Genovese MC, Moreland LW (2001) Demyelinating and neurologic events reported in association with tumor necrosis factor alpha antagonism: by what mechanisms could tumor necrosis factor alpha antagonists improve rheumatoid arthritis but exacerbate multiple sclerosis? Arthritis Rheum 44:1977–1983.

Scherbel U, Raghupathi R, Nakamura M, Saatman KE, Trojanowski JQ, Neugebauer E, Marino MW, McIntosh TK (1999) Differential acute and chronic responses of tumor necrosis factor-deficient mice to experimental brain injury. Proc Natl Acad Sci USA 96:8721–8726.

Sicotte NL, Voskuhl RR (2001) Onset of multiple sclerosis associated with anti-TNF therapy. Neurology 57:1885–1888.

Sriram S, Rodriguez M (1997) Indictment of the microglia as the villain in multiple sclerosis. Neurology 48:464–470.

Suvannavejh GC, Lee HO, Padilla J, Dal Canto MC, Barrett TA, Miller SD (2000) Divergent roles for p55 and p75 tumor necrosis factor receptors in the pathogenesis of MOG(35–55)-induced experimental autoimmune encephalomyelitis. Cell Immunol 205:24–33.

Turnley AM, Morahan G, Okano H, Bernard O, Mikoshiba K, Allison J, Bartlett PF, Miller JF (1991) Dysmyelination in transgenic mice resulting from expression of class I histocompatibility molecules in oligodendrocytes. Nature 353:566–569.